

## Modelling the spatial distribution of the annihilation emission of positrons produced by $^{26}\text{Al}$

A. Alexis<sup>\*1</sup>, P. Jean<sup>1</sup>, P. Martin<sup>2</sup>, K. Ferrière<sup>3</sup>, N. Guessoum<sup>4</sup> and P. von Ballmoos<sup>1</sup>

<sup>1</sup>Centre d'Etude Spatiale des Rayonnements, CNRS/Université de Toulouse, INSU  
9 avenue du Colonel Roche, BP 44346, 31028 Toulouse, France

<sup>2</sup>Max Planck für extraterrestrische Physik, Postfach 1312, 85741 Garching, Germany

<sup>3</sup>LATT, CNRS/Université de Toulouse, 14 avenue Edouard Belin, 31400 Toulouse, France

<sup>4</sup>American University of Sharjah, College of Arts & Sciences, Physics Department  
PO Box 26666, Sharjah, UAE

E-mails: alexis@cesr.fr, jean@cesr.fr,  
pierrick.martin@obs.ujf-grenoble.fr,  
ferriere@ast.obs-mip.fr, nguessoum@aus.edu,  
pvb@cesr.fr

We modelled the spatial and spectral distributions of the annihilation emission induced by positrons that are released in the decay of  $^{26}\text{Al}$  nuclei in the Galactic disk. This was carried out through Monte Carlo simulations that take into account the propagation of positrons in the interstellar medium (ISM). The  $^{26}\text{Al}$  distribution was assumed to follow the free-electron spatial distribution given by Cordes & Lazio (2001). The gas distribution is based on the model given by Ferrière (1998). Due to uncertainties in the regime of positron transport in the ISM, we tested several propagation modes. When scattering off MHD waves is ignored, positrons annihilate mainly in the warm phases of the ISM, whereas they annihilate almost exclusively ( $\sim 96\%$ ) in the warm ionized phases when they can scatter off MHD waves. Moreover, a slight asymmetry in the 511 keV annihilation emission is observed toward negative longitudes in the two types of simulations.

8th INTEGRAL Workshop “The Restless Gamma-ray Universe”  
September 27-30 2010  
Dublin Castle, Dublin, Ireland

---

\*Speaker.

## 1. Introduction

The origin of Galactic positrons remains unclear. Observations of the 511 keV emission by SPI-INTTEGRAL (Knödlseeder et al. 2005) showed that the disk emission could be explained by radioactive decay of  $^{26}\text{Al}$  and  $^{44}\text{Ti}$  produced in massive stars, assuming positrons annihilate close to their source. However, positrons are expected to propagate. Understanding positron propagation mechanisms is thus the key to understanding the annihilation emission's spatial distribution as well as the origin of positrons. Here, we present a propagation model of positrons in the Galactic disk. We run Monte Carlo simulations of positrons produced by  $^{26}\text{Al}$ , which should be the dominant source of positrons in the disk. We discuss the results obtained.

## 2. Modelling positron transport in the Galactic disk

To model the propagation of  $^{26}\text{Al}$  positrons in the disk, we had to carefully model the ISM of the Galaxy (see Sec. 2.1), the positron physics (see Sec. 2.2), and propagation modes for MeV positrons (see Sec. 2.3). Due to large uncertainties in the magnetic field and gas distribution in the bulge ( $\leq 1.5$  kpc), we disregarded positrons entering this region, an issue which will be dealt with in the future.

### 2.1 The ISM

The structure of the Galactic magnetic field (GMF) is often described with two components: the regular Galactic magnetic field,  $\vec{B}_0$ , and the turbulent Galactic magnetic field,  $\vec{\delta B}$ . These two components are probed with measurements of the total and polarized synchrotron emission and Faraday rotation of pulsars and extragalactic sources. Overall, the total GMF is poorly known, but a recent study (Jaffe et al. 2010) gives us a 2D GMF model from a new parametric method simulating some observables. We use the  $\vec{B}_0$  described in Jaffe et al. (2010). The configuration of this coherent spiral arm magnetic field model in the Galactic plane is shown in Figure 1. In order to obtain a complete 3D model of the  $\vec{B}_0$ , we assume that the spiral field strength decreases exponentially above and below the Galactic plane with two scale heights (1 kpc and 4 kpc) as described by Alvarez-Muñiz et al. (2002).

The  $\vec{\delta B}$  is simulated using the plane wave approximation method described by Giacalone & Jokipii (1994). Magnetic field fluctuations follow a Kolmogorov spectrum and have a maximum turbulent scale of  $\lambda_{\text{max}} \simeq 10\text{-}100$  pc in the hot and the warm phases and  $\lambda_{\text{max}} \simeq 1\text{-}10$  pc in the cold neutral and the molecular phases (Jean et al. 2009). In previous studies (Prantzos 2006, Jean et al. 2009), the ratio  $\delta B/B_0$  was assumed to be constant throughout the Galaxy. We here allow this ratio to vary in space with  $\delta B/B_0$  increasing smoothly from 1 in interarm regions to 2 on the arm ridges (see Jaffe et al. 2010). For this first study, we did not assume a vertical cut-off of the turbulent component.

During propagation, a positron interacts with the gaseous matter of the ISM and loses energy (see Sec. 2.2). It is therefore necessary to assume some Galactic distribution of the interstellar gas. Here, we adopt the model given by Ferrière (1998), where the ISM, composed of hydrogen and  $\simeq 9\%$  of helium<sup>1</sup>, is described by five phases: the molecular medium (MM), the cold neutral

<sup>1</sup>Amounts of heavier elements are negligible.

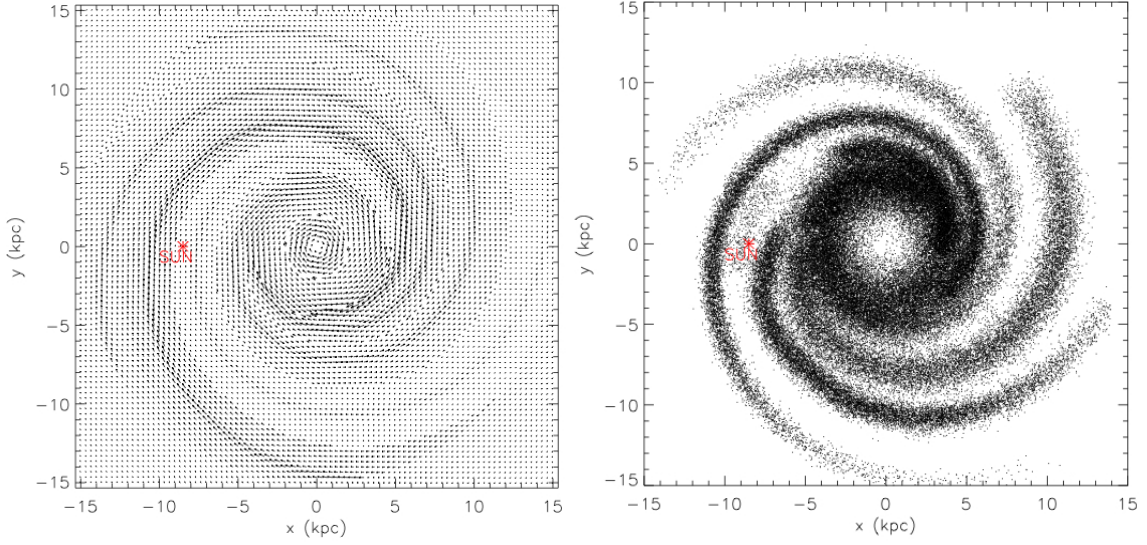


Figure 1: Left panel: the  $\vec{B}_0$  configuration in the Galactic plane (Jaffe et al. 2010). The vectors indicate the direction of the field, and their length is proportional to its amplitude. Right panel: a random distribution of 100000  $^{26}\text{Al}$  positrons in the Galactic plane using Cordes & Lazio (2001).

medium (CNM), the warm neutral medium (WNM), the warm ionized medium (WIM), and the hot ionized medium (HIM). This model gives the space-average density  $\langle n_i \rangle$  of each ISM phase. However, positrons propagate in gases with true densities. We derived the true density  $n_i$  of each phase using the method described in Jean et al. (2005).

We assume that a positron crosses into a different ISM phase when the distance it travels is greater than the typical size of the phase it was in. The new phase is chosen randomly (by Monte Carlo), where the probability of entering a new phase  $i$  is equal to its volume filling factor  $\phi_i$  ( $\phi_i = \langle n_i \rangle / n_i$ ). The size of the new phase  $i$  is selected randomly in the range of typical sizes of this phase (see Table 1 of Jean et al. 2009).

## 2.2 Positron physics

The radioisotope  $^{26}\text{Al}$  decays with a lifetime of  $\sim 1$  Myr, emitting a gamma-photon at 1809 keV. 82% of the decays are accompanied by a positron with a mean energy of  $\simeq 0.5$  MeV. We randomly choose the initial energy of each positron by a numerical bijection method in the energy spectrum of positrons emitted by  $^{26}\text{Al}$ . We assume that the  $^{26}\text{Al}$  follows the free-electron spatial distribution of Cordes & Lazio (2001), since Knödlseher et al. (1999) showed that the gamma-ray emission at 1809 keV is strongly correlated with free-free emissions from electrons. Figure 1 presents a sample of initial positions of  $^{26}\text{Al}$  positrons produced in the disk. The bulge is not modelled in this study, thus the bulge component of Cordes & Lazio (2001) is not taken into account.

After being injected into the ISM in random directions, positrons propagate in the Galaxy until they annihilate directly with an electron or via Positronium (Ps) formation. Before annihilating, MeV positrons undergo continuous energy loss processes, such as Coulomb collisions with electrons in the ionized phases or may undergo binary interactions, such as excitation and ioniza-

		Simulation with collisional transport only		Simulation with collisional transport and scattering off mhd waves	
Sky regions ( $ b  < 10^\circ$ )		$-50 < l < 0$	$0 < l < 50$	$-50 < l < 0$	$0 < l < 50$
ISM annihilation phase fractions (%)	Molecular	1.4	1.6	0.15	0.2
	Cold Neutral	11.1	9.5	0.95	0.7
	Warm Neutral	30	29.4	3.2	2.8
	Warm Ionized	55.75	58.2	95.1	96
	Hot Ionized	1.75	1.3	0.6	0.3
511 keV Galactic flux ( $10^{-4}$ ph cm $^{-2}$ s $^{-1}$ )		1.17	1.07	1.63	1.3
Positron mean distance travelled (kpc)		1.5		0.23	
Positron fraction entering the bulge (%)		1.24		0.4	

Table 1: Results for each simulation in two sky regions:  $-50^\circ < l < 0^\circ$  and  $0^\circ < l < 50^\circ$  ( $|b| \leq 10^\circ$ ).

tion of atoms and molecules in the neutral phases. The latter interactions occur randomly in the ISM and are determined by a Monte Carlo method which includes the cross sections of these processes. During these collisions, positrons also suffer pitch angle scattering, which we model as in Jean et al. (2009). All continuous energy loss processes are also taken into account.

The simulation stops when the positron annihilates in flight or when its energy drops below a threshold energy that we set to 100 eV, below which the distance traveled by a positron is small compared to the size of the phase. Thus we can consider that positrons annihilate at that location in the Galaxy. We estimate the annihilation emission (511 keV, ortho-Ps $^2$ ) fluxes as function of Galactic coordinates, the Ps formation fraction in that current phase, the distance between that location and the Sun, and the mass of  $^{26}\text{Al}$  within the Galaxy ( $\simeq 2.8 M_\odot$ ).

### 2.3 Propagation modes

Understanding the propagation mechanisms of MeV positrons is a key point for solving the mystery of the Galactic positrons' origin. Following Jean et al. (2009), we modelled two propagation modes: the collisional regime, and the scattering off MHD waves. In the first mode, positrons propagate along steady state magnetic field lines, and their pitch angles change in collisions with gas particles. Positrons may also scatter off MHD waves when they satisfy the Landau-synchrotron resonance condition. Jean et al. (2009) showed that positrons could only interact with Alfvén waves in ionized phases because turbulent cascades initiated at large scales ( $\gtrsim 100$  pc) in these phases could keep transferring energies down to scales lower than the Larmor radii of MeV positrons. We modelled this propagation mode in an anisotropic way because in our model, the  $\overrightarrow{\delta B}$  overlays the  $\overrightarrow{B}_0$ , so that the scattering of positrons will be more parallel than orthogonal to the  $\overrightarrow{B}_0$ . Using the method presented in Wommer et al. (2008), we computed parallel and orthogonal diffusion coefficients for positron energies in the range  $0.06 \text{ MeV} < E < 1 \text{ MeV}$  and magnetic field strengths in the range  $0.25 \mu\text{G} < B < 4 \mu\text{G}$ . These coefficients are then used to calculate the displacement of the positron. Thus scattering off MHD waves acts like a random walk for the positron. However, this propagation mode remains uncertain because observations of turbulence amplitudes at these

<sup>2</sup>One of the two Ps states, ortho-Ps decays into 3 photons of energies totaling 1022 keV.

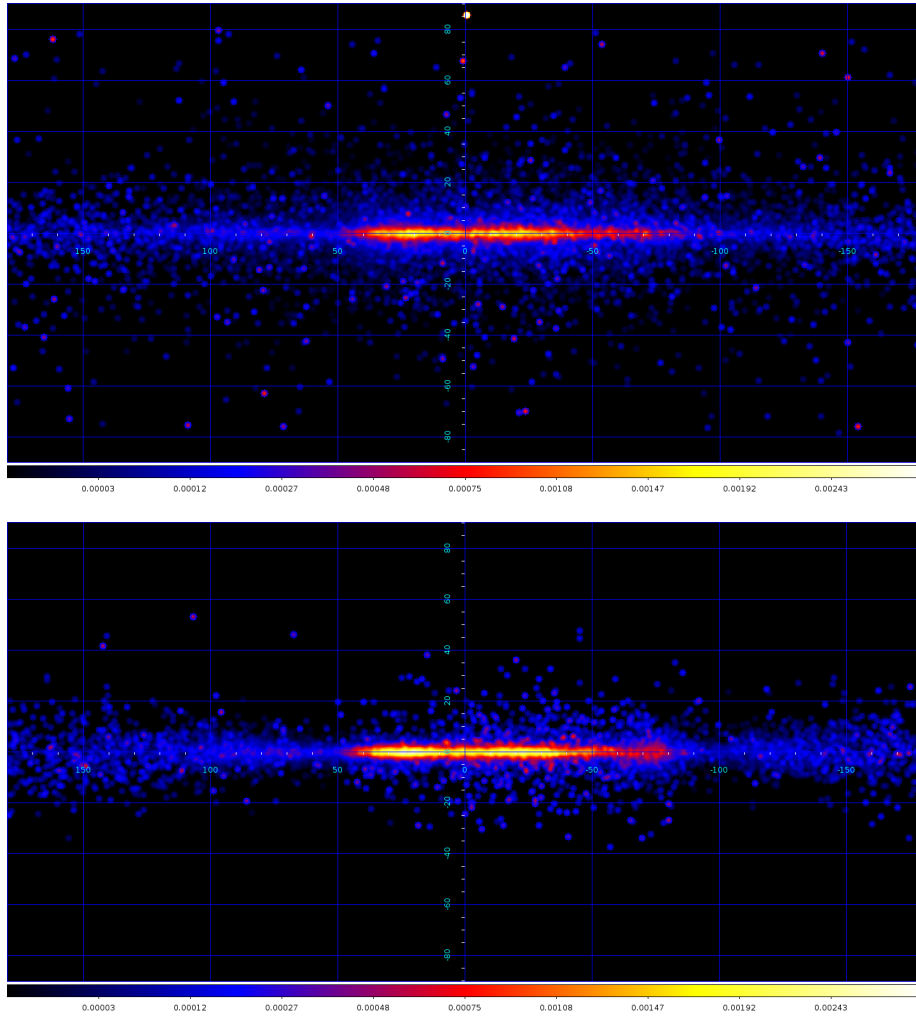


Figure 2: Sky maps of the 511 keV  $e^+e^-$  annihilation line emission for the simulations (in  $\text{ph cm}^{-2}\text{s}^{-1}\text{sr}^{-1}$ ) without (top) and with (bottom) scattering off MHD waves.

scales do not exist. Therefore, we performed two kinds of simulations : with and without scattering off Alfvén waves.

### 3. Results and discussion

We simulated 20000 positrons released in the HIM, and we obtained sky maps of  $e^+e^-$  annihilation flux (see Figure 2), as well as information on the propagation and annihilation of positrons (see Table 1). The Monte Carlo simulation stops when positrons enter the bulge, escape the Galaxy ( $R_{\text{positron}} \geq 15 \text{ kpc}$ ), annihilate directly in flight or have their energy dropping below 100 eV.

When positrons propagate only in the collisional mode, 90% of the annihilations occur at  $|b| \leq 7^\circ$ , whereas when scattering off MHD waves is taken into account, positrons are more confined to the Galactic plane ( $|b| \leq 3^\circ$ ). In both simulations, the bulk of the emission is concentrated in the longitude range  $|l| \leq 50^\circ$ , in agreement with the extent measured by SPI (Weidenspointner et al. 2008). When positrons scatter off MHD waves, positrons annihilate almost exclusively

( $\sim 96\%$ ) in the WIM. In this phase, positrons meet the resonance condition, and they scatter off MHD waves for a long time while they lose energy down to 100 eV. Their behaviour is similar in the HIM, but since the density of the HIM is very low, positron energy losses are extremely small and positrons can escape the HIM with a high probability of entering a warm phase, due to the large volume filling factor of this phase. When positrons propagate in the collisional mode only, they annihilate mainly in the warm phases ( $\sim 55\%$  in the WIM and  $\sim 30\%$  in the WNM) with a small fraction in the CNM.

Although positrons travel on average  $\sim 1.5$  kpc in the collisional mode, the annihilation emission seems to follow the source spatial distribution, because positrons propagate along GMF lines which themselves follow nearly the spiral arms, which is where the  $^{26}\text{Al}$  decays. A negligible fraction ( $\lesssim 1.2\%$ ) of positrons enter the Galactic Bulge (see Table 1); this excludes the possibility that positrons produced by  $^{26}\text{Al}$  contribute to the large bulge-to-disk luminosity ratio of the 511 keV line measured with SPI. However, we do not use a poloidal magnetic field orthogonal to the Galactic plane, as done by Prantzos (2006), who finds that positrons produced by type-Ia supernovae in the disk may be transported, via this type of field, into the bulge. The exact magnetic structure needs to be investigated in order to fully understand the propagation of positrons across the Galaxy.

The total flux at 511 keV is in agreement with what we expect for positrons produced by  $^{26}\text{Al}$  (i.e.  $\sim 5 \times 10^{-4}$  ph cm $^{-2}$ s $^{-1}$ , Knödlseider et al. 2005) assuming positrons annihilate close to their production sites. We obtain  $\sim 6.9 \times 10^{-4}$  and  $\sim 5.3 \times 10^{-4}$  ph cm $^{-2}$ s $^{-1}$  for the simulations with and without scattering off MHD waves, respectively. We thus conclude that  $^{26}\text{Al}$  seems to be able to explain the Galactic disk emission. Moreover, the ratios of the simulated fluxes (see Table 1) at negative and positive longitudes is in agreement with the asymmetry measured by Wang et al. (2009) for the  $^{26}\text{Al}$  1809 keV line flux ( $F_{l<0}/F_{l>0} \simeq 1.3 \pm 0.2$ ). We obtain a ratio  $\simeq 1.25$  and  $\simeq 1.1$  for the simulations with and without the scattering off MHD waves, respectively. This asymmetry is due to the asymmetric distribution of free electrons in the inner regions (Cordes & Lazio 2001). In future works, we will consider positrons produced by other sources (type-Ia supernovae,  $^{44}\text{Ti}$ ).

## References

- [1] Alvarez-Muñiz, J., Engel, R. & Stanev, T., 2002, ApJ, 572, 18
- [2] Cordes, J.M., & Lazio, T. J. W., 2002, preprint at <http://arXiv.org/astro-ph/0207156>
- [3] Ferrière, K., 1998, ApJ, 503, 700
- [4] Giacalone, J., & Jokipii, J. R., 1994, ApJ, 430, L137
- [5] Jaffe, T., et al., 2010, MNRAS, 401, 1013
- [6] Jean, P., et al., 2009, A&A, 508, 1099
- [7] Knödlseider, J., 1999, ApJ, 510, 915
- [8] Knödlseider, J. et al., 2005, A&A, 441, 513
- [9] Prantzos, N., 2006, A&A, 449, 869
- [10] Wang, W., et al., 2009, A&A, 496, 713
- [11] Weidenspointner, G., et al., 2008, Nature, 451, 159
- [12] Wommer, E., Melia, F., Fatuzzo, M., 2008, MNRAS, 387, 987